

Table of contents:

Material and methods	page 1–5
Statistical analyses	page 5–9
Code and data availability	page 9
Supplemental figures	page 10–16
Supplemental table	page 17
Supplemental references	page 18
Acknowledgements	page 19

Inactivation of H5N1 virus in raw milk at 63 and 72 degrees Celsius

Franziska Kaiser¹, Dylan H. Morris², Arthur Wickenhagen¹, Kwe Claude Yinda¹, Emmie de Wit¹, James O. Lloyd-Smith², Vincent J. Munster¹

1. Laboratory of Virology, Division of Intramural Research, National Institute of Allergy and Infectious Diseases, National Institutes of Health, Hamilton, MT, USA
2. Department of Ecology and Evolutionary Biology, University of California, Los Angeles, Los Angeles, CA, USA

Materials and methods

Laboratory experiments

Regulatory Compliance

This work was performed in the NIAID Rocky Mountain Laboratories maximum containment facility. This facility and the work with HPAI H5N1 virus has been approved by the Federal Select Agent Program of the CDC Division of Regulatory Science and Compliance (DSAT). The work presented here was deemed non-dual use by the NIH DURC committee, as it does not enhance the harmful consequences of the agent, nor does it disrupt the effectiveness of immunization, nor does the work confer resistance to prophylactic or therapeutic inventions, nor does it increase the stability or transmissibility of the agent, nor does it change the tropism of the agent, nor does it pertain to the generation of an extinct agent.

Cells

Madin-Darby canine kidney (MDCK) cells (Erasmus Medical Center, Rotterdam), were cultured in modified essential medium (MEM) supplemented with 10% fetal bovine serum (FCS), 50 IU/ml penicillin, 50 µg/ml streptomycin, 2 mM glutamine, 0.75 mg/ml sodium bicarbonate, and nonessential amino acids (all Gibco).

Viruses

HPAI H5N1 A/mountain lion/MT/1/2024 (clade 2.3.4.4b, EPI_ISL_19083124) was isolated from the lungs of a mountain lion found dead in Montana in February 2024 and passaged once in MDCK cells. Overall amino acid identities between this isolate and a HPAI H5N1 A/dairy cow/Texas/24-008749-001-original/2024 clade 2.3.4.4b, EPI_ISL_19014384) currently circulating in US dairy herds are: PB2 (97.8 %), PB1 (99.0 %), PA (99.7%), HA (100%), NP (99.0 %), NA (99.4%), M1 (100%), M2 (100%) and NS1 (99.1 %).

Quantitative real-time RT-PCR (qRT-PCR).

Nucleic acid extraction was performed using the QIAamp Viral RNA Kit (Qiagen) according to the manufacturer's instructions on the QIAcube HT automated system (Qiagen). The extraction was performed on 70 µl of original sample volume and eluted in a volume of 75 µl. A one-step real-time RT-PCR targeted at the matrix gene of influenza A virus was performed using the Taqman fast-virus 1-step master-mix (Thermo Fischer Scientific) according to instructions of the manufacturer using the primers and probe in 20µl reactions with the TaqMan Fast Virus 1-Step kit, as previously described¹. The assay was conducted on a QuantStudio 3 Flex Real-Time PCR System (Applied Biosystems) and the following cycler settings: 50 °C for 10 min, 95 °C for 5 min and 40 cycles of 95 °C for 10 s and 60 °C for 30 s. RNA standards with known copy numbers were used to calculate copy numbers/ml.

Virus titration

Virus titration was performed by endpoint dilution in MDCK cells. MDCK cells were inoculated with tenfold serial dilutions of milk spiked with virus. One hour after inoculation, cells were washed three times with phosphate-buffered saline (PBS) and grown in infection medium (MEM supplemented with 50 IU/ml penicillin, 50 µg/ml streptomycin, 2 mM glutamine, 0.75 mg/ml sodium bicarbonate, nonessential amino acids, and 5 µg/ml trypsin). Three days after inoculation, the supernatants of infected cell cultures were tested for agglutination activity using turkey red blood cells as an indicator of infection of the cells.

Experimental considerations

The experimental conditions evaluated were based on the most common method of pasteurization in the United States today, which are the 63 °C for 30 minutes and the 72 °C, 15 seconds High Temperature Short Time (HTST) pasteurization². The titer of 10⁶ TCID₅₀/ml was chosen to allow robust inference of decay rates, but it also is within the range of titers reported by research groups investigating infectious titers of HPAI H5N1 within raw milk taken from infected cows: 10⁶ and 10⁸ TCID₅₀/ml (personal communications). In addition, Cycle Threshold (CT) values reported in pasteurized retail milk, ranged around 29-31, whereas

in our study the CT value ranged between 25 and 28, where 3 CT units is an 8 fold difference in copy numbers. This suggests that the titer used here would potentially represent the upper end of what dairy processors could encounter in real-life³, though we note that real-life dairy supplies would be diluted considerably by mixing of milk from infected and uninfected cows

Experimental design for heat inactivation at 63 °C

Untreated raw cow milk was spiked with A/mountain lion/MT/1/2024 to achieve a 10^6 TCID₅₀/ml concentration. Spiked milk was aliquoted into 1.5 ml reaction tubes with a volume of 750 µl per tube. Closed tubes with cooled milk-virus suspension were placed in a pre-heated and temperature-controlled thermomixer (Eppendorf), filled with water to ensure efficient heat-transfer. Tubes were removed from the heat block 20, 40 seconds, and 1, 1.5, 2, 3, 5, 7.5, 10, 20, and 30 minutes after the milk reached 63 °C, and immediately put on ice. Temperature was measured with an analog partial immersion thermometer, and the aliquots took 48 s to heat up to 63 °C. After reaching the preset incubation timepoints, samples were rapidly cooled in ice-water mixture and remained on ice until titration. Results were compared to non-heat-treated milk at T0. All experiments were performed in triplicate, and different timepoints correspond to different reaction tubes (i.e. no tubes were sampled longitudinally).

Experimental design for heat inactivation at 72 °C

As a first attempt, the same experimental set-up used for the 63 °C heat inactivation was utilized to test virus inactivation at 72 °C, with sampling timepoints after 5, 10, 15, 40 seconds, and 1, 2, 3 minutes. Temperature of the heating block and samples was confirmed using an analog partial immersion and digital probe thermometer, respectively. The milk-virus suspension in 750 µl aliquots reached 72 °C after 58 s. After 5 s at 72 °C $10^{1.1}$ [95% CrI $10^{0.5}$, $10^{1.6}$] TCID₅₀/ml infectious virus was detected. One out of three replicates was positive. Subsequent timepoints had no positive wells for any of the three replicate tubes. Due to the absence of infectious virus after the target temperature was reached, save for one replicate tube at the first timepoint, a half-life calculation for infectious virus at 72 °C was not feasible, as these data suggested that much of the inactivation had happened during the pre-heating, i.e. prior to the milk reaching 72 °C.

To minimize temperature ramp-up time and virus inactivation during this period, a second experiment was performed at 72 °C. 496 µl aliquots of raw milk were heated up to 72 °C in a digital temperature-controlled thermomixer with 400 rpm. After the milk reached 72 °C, 4 µl of virus stock were added to reach a titer of 10^6 TCID₅₀/ml. Samples were incubated in the thermomixer with 400 rpm for 0, 5, 10, 15, 20, 25, and 30 s and immediately transferred to an ice-water mixture for rapid cooling. All experiments were performed

in triplicate, and different timepoints correspond to different reaction tubes (i.e. no tubes were sampled longitudinally).

Evaluation of qRT-PCR positivity after heat treatment

In a separate experiment, 750 μl aliquots of milk spiked with 10^6 TCID₅₀/ml were exposed to 63 °C for 30 min according to the experimental design for the 63 °C heat treatment described previously. Additionally, one 750 μl aliquot was heated up to 72 °C for 15 s. The qRT-PCR results from these samples were compared to those from a non-treated milk-virus suspension, that was kept at room temperature for 30 min. The observed reduction in detectable H5N1 genetic material was minimal for all groups, with the highest decrease for the 30 min at 63 °C group (mean 7.14 log₁₀ copies/ml compared to 7.6 log₁₀ copies/ml in the start suspension; Supplemental Figure 2). All experiments were performed in triplicate.

Statistical analyses

Inference models

We inferred individual sample titers and experiment half-lives from raw endpoint titration well data in a Bayesian framework, as previously described⁴. The only differences from the approach taken in that paper were:

1. In this work, we used NumPyro⁵ and Python 3 rather than Stan and R to specify and fit the Bayesian model.
2. We chose prior distributions appropriate to the experiment at hand and assessed their appropriateness with prior predictive checks.

Note that the individually-inferred titer posteriors represent our measured values. They are a Bayesian version of the endpoint titer estimates one would obtain by an approximate method such as Spearman-Kärber or Reed-Muench, but with the uncertainty quantification that comes from inferring the full posterior distribution from the prior and likelihood (whereas traditional methods yield a point estimate without uncertainty). Where we report point estimates, these are the posterior medians.

Brief description of the likelihood

As previously described⁴, we modeled individual titration well positivity according to a Poisson single-hit process. That is, if a set of susceptible cells are inoculated with a solution containing infectious virions, the number of virions that productively infect cells will be approximately Poisson distributed with a mean given by the concentration of virions in the original sample multiplied by the per-virion cell infection probability. If any of the virions successfully invade a cell and replicate (a “single hit”) there will be evidence of cellular infection, so the probability that an inoculated well of cells is positive for virus infection can be modeled as the probability that a Poisson random variable is greater than or equal to 1. This same probabilistic model underlies approximate titer computation methods such as the Spearman-Kärber method. By measuring the underlying mean in units of 50% probability tissue culture infectious dose (TCID₅₀), we can abstract away the per virion infection probability.

It follows that the probability of observing a positive well $Y = 1$ given a true underlying sample virion concentration ν (in units of \log_{10} TCID₅₀ per unit volume) diluted by a factor of 10^d and inoculated in a volume of z is:

$$P(Y = 1 \mid \nu, d, z) = 1 - \exp[-\ln(2) * z * 10^{(\nu-d)}]$$

$\exp[x] = e^x$ denotes the exponential function. The factor of $\ln(2)$ comes from the fact that the units of ν are \log_{10} TCID₅₀ per unit volume, so the probability of a positive well when exactly 1 TCID₅₀ is inoculated (i.e. $z * 10^{(\nu-d)} = 1$) must be 0.5.

The probability of observing a negative well $Y = 0$ is:

$$P(Y = 0 \mid \nu, d, z) = \exp[-\ln(2) * z * 10^{(\nu-d)}]$$

To compute an overall likelihood of observing a series of well values (i.e. $Y_1=y_1, Y_2=y_2, \dots Y_n=y_n$) given a true underlying titer ν and a series of dilution factors $d_1, d_2, \dots d_n$ it suffices to take the product of the individual well conditional probabilities, under the assumption that the individual well inoculations are conditionally independent trials given ν :

$$P(Y_1=y_1, Y_2=y_2, \dots Y_n=y_n \mid \nu, d_1, \dots d_n, z) = P(Y_1=y_1 \mid \nu, d, z) * P(Y_2=y_2 \mid \nu, d, z) * \dots P(Y_n=y_n \mid \nu, d, z)$$

To infer individual titers independently, we applied this likelihood along with a prior to infer all titers, where the k^{th} titer ν_k has one or more associated titration wells i ($i=1,2,\dots$), with virus positivity/negativity values y_{ki} ($y_{ki}=1$ for positive, $y_{ki}=0$ for negative).

To infer half-lives, we model virus decay in each condition j at a rate l_j . Each titrated sample v_{kj} from condition j begins at an inferred $t = 0$ titer value $v_{kj}(0)$ and decays exponentially at a rate $l_j \log_{10} \text{TCID}_{50}$ per unit time until it is sampled at time t_{kj} . Because we are working in \log_{10} units, this exponential decay expression is linear:

$$v_{kj}(t_{kj}) = v_{kj}(0) - l_j t_{kj}$$

To infer l_j , and the $v_{kj}(0)$, we use the same likelihood function detailed above to describe raw well positivity/negativity for the i^{th} associated titration well y_{kji} given an underlying titer $v_{kj}(t)$. To model the $v_{kj}(0)$ values, we use a hierarchical approach. The $v_{kj}(0)$ are Normally distributed about an inferred condition-specific mean $\langle v_0 \rangle_j$ with an inferred condition-specific standard deviation σ_j :

$$v_{kj}(0) \sim \text{Normal}(\langle v_0 \rangle_j, \sigma_j)$$

Note that as the $v_{kj}(0)$ are \log_{10} titers, this implies the initial virus concentrations for specific titrated samples are log-normally distributed on the natural scale.

This hierarchical approach allows us to account for the fact that each titrated sample is measured only once, and so potential variability in the $t = 0$ values $v_{kj}(0)$ must be accounted for when attempting to infer the (shared) exponential decay rate l_j .

Model checking

We assessed appropriateness of prior distribution choices with prior predictive checks, confirming that all priors were largely agnostic across the range of biologically plausible values. Prior predictive checks are shown in Supplementary Figure 2

Prior distributions

In the following specification, Normal distributions are parameterized as Normal(mean, standard deviation) and Positive Truncated Normal distributions (i.e. Normal shaped density, but truncated to the interval $(0, \infty)$ and renormalized to sum to 1) are parameterized in terms of the mode and standard deviation of the underlying un-truncated normal as PosNormal(mode, standard deviation).

We used the following priors for the results presented in the main text:

We placed a very weakly informative Normal prior on the individual titers v_i in units of \log_{10} TCID₅₀ per mL:

$$v_i \sim \text{Normal}(0, 10)$$

We used weakly informative prior for the experiment-specific mean starting \log_{10} titers $\langle v_0 \rangle_j$ based on the target stock titer:

$$\langle v_0 \rangle_j \sim \text{Normal}(5, 2)$$

We placed a weakly informative Positive-Truncated Normal prior on the standard deviation σ_j of the distribution of individual sample initial titers about the mean, which allows either for minimal or for considerable variation in the individual initial sample titers about the mean.

$$\sigma_j \sim \text{PosNormal}(0, 0.25)$$

We placed a conservative (mode of 10 min) but weakly informative (considerable dispersion) prior on the infectious virus log (base e) half-life in minutes under heat treatment:

$$\ln(h_j) \sim \text{Normal}(\ln(10), \ln(20))$$

Prior sensitivity analysis

To measure sensitivity of our results to the choices of priors, we re-ran the analyses using several other choices for the prior hyperparameters. Results are shown below, in each case with a version of the Main Text Figure and the prior predictive check figure (Figure S2) with the given priors, noted explicitly in the figure. N denotes the normal distribution and N^+ the positive-truncated Normal. The results are shown in Figures S3–S7. Allowing for less variation in the individual sample $t=0$ values $v_{kj}(0)$ by forcing σ_j to be small produces more certain estimates of the half-life, while allowing for more variation produces less certain ones, but overall the results are qualitatively and quantitatively robust to the choice of priors, suggesting the data constrain the values strongly. When most prior mass is far from the observed data, as in figure S6, the posterior estimates are still pulled strongly toward the observations. When we encourage the model to use a strongly dispersed initial titer value varying across multiple logs 10 (Figure S7), the model considers somewhat longer half-lives *a posteriori* more plausible than in our main text estimates, but the qualitative result that many logs 10 of virus are lost within the first few minutes is preserved.

Computational details

We inferred posterior distributions jointly for all parameters by drawing Markov Chain Monte Carlo (MCMC) using a No-U-Turn Sampler (NUTS) approach; NUTS is a form of Hamiltonian Monte Carlo. We ran 4 MCMC chains from random initial conditions for each Bayesian analysis, with 1000 warmup iterations and 1000 sampling iterations per chain, a target acceptance probability of 0.85, and a maximum tree depth of 10.

We assessed MCMC convergence by examining trace plots and by consulting convergence diagnostic statistics (Gelman-Rubin R-hat values for all parameters < 1.01 , all bulk and tail effective sample sizes greater than 1000, and no divergent transitions after warmup for any MCMC chain).

To improve reproducibility, we fixed seed values for all pseudorandom number generators used.

Code and data availability

Code and data to reproduce the Bayesian estimation results and produce corresponding figures are archived online on Zenodo and made available on Github at <https://github.com/LloydSmithLab/h5n1-inactivation>. This repository also includes tables of inferred values and MCMC convergence diagnostics. Raw data is available at 10.6084/m9.figshare.25880209.

Supplemental Figures

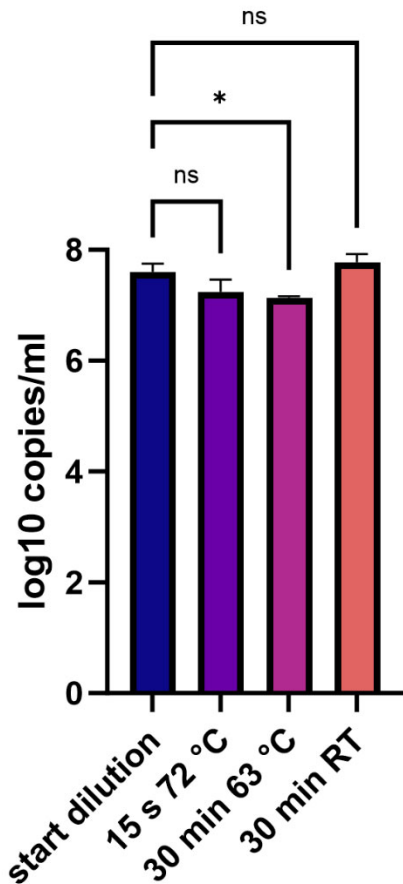


Figure S1. H5N1 copy numbers by qRT-PCR after heat treatments. Raw milk samples (750µl aliquots) with 10^6 TCID₅₀/ml were exposed to the two investigated heat treatments (15 s exposure to 72 °C, and 30 min to 63 °C) and compared to a non-treated control (30 min at room temperature). The bar graph is depicting the median and 95% CI. Significance was tested by one-way ANOVA followed by Tukey's multiple comparison test. $p < 0.05$ is marked with asterisk.

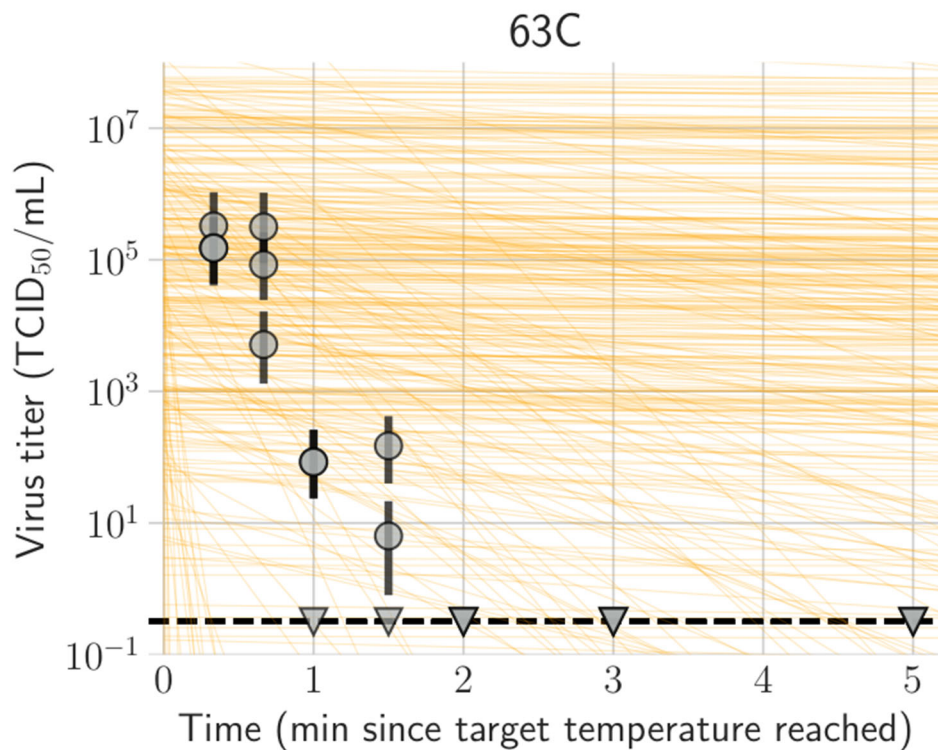
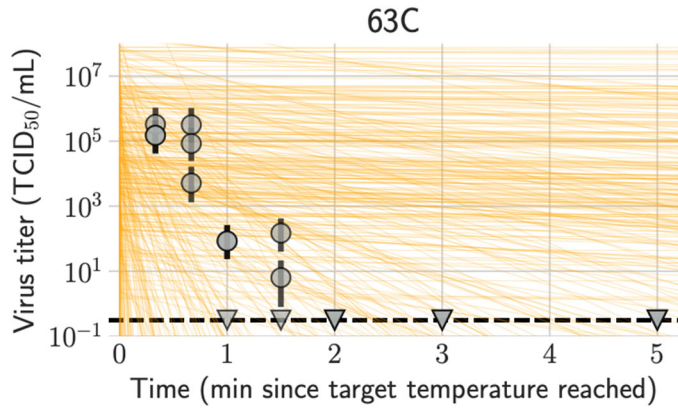


Figure S2: Prior predictive checks for half-life model. This plot has the same form as panel A of the Main Text Figure, but with predicted decay lines drawn from the joint prior distribution of half-lives and intercepts rather than inferred from the data. The wide coverage of lines show that the prior was indeed conservative, and allowed for a range of inactivation rates, including inactivation substantially slower or faster than what was inferred from the data.

We assessed goodness-of-fit of our half-life inference model by plotting posterior predictions of titer from the half-life inference model against the individually-inferred titer values (Main Text Figure, panel A).



$$\ln(h_j) \sim \mathcal{N}(\ln(1), \ln(50)),$$

$$\langle v_0 \rangle_j \sim \mathcal{N}(5, 2),$$

$$\sigma_j \sim \mathcal{N}^+(0, 0.25)$$

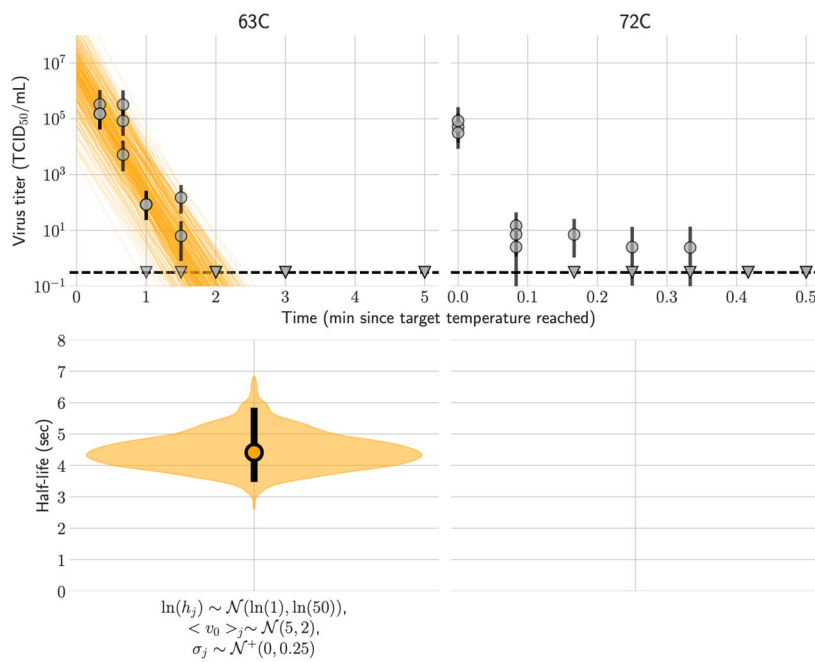
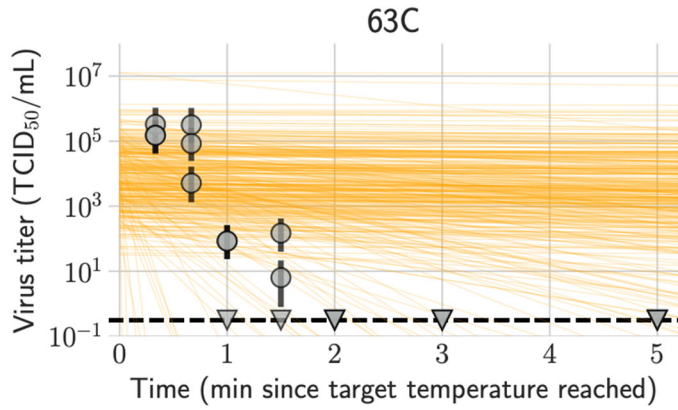


Figure S3: Prior predictive check and version of main text figure with first set of alternative half-life priors. Version of Figure S2 and main text figure, but with prior choices changed as indicated.



$$\ln(h_j) \sim \mathcal{N}(\ln(10), \ln(20)),$$

$$\langle v_0 \rangle_j \sim \mathcal{N}(4, 1),$$

$$\sigma_j \sim \mathcal{N}^+(0, 0.05)$$

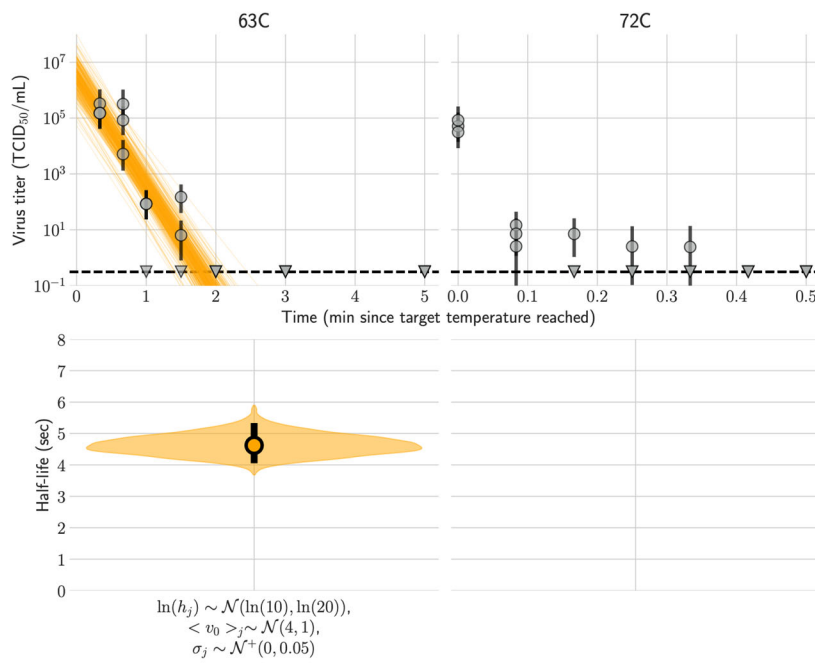
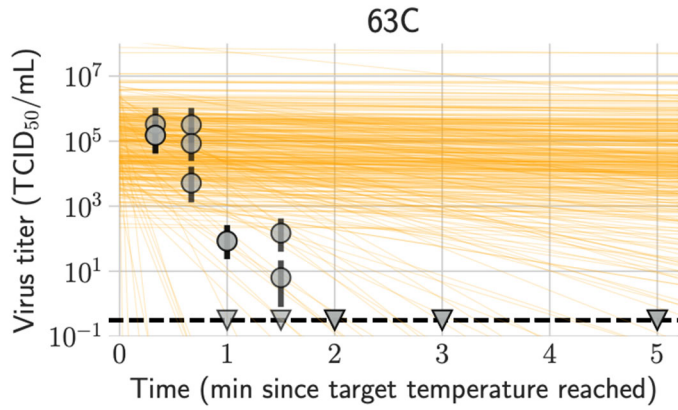


Figure S4: Prior predictive check and version of main text figure with first set of alternative half-life priors. Version of Figure S2 and main text figure, but with prior choices changed as indicated.



$$\ln(h_j) \sim \mathcal{N}(\ln(10), \ln(20)),$$

$$\langle v_0 \rangle_j \sim \mathcal{N}(5, 1),$$

$$\sigma_j \sim \mathcal{N}^+(0, 0.125)$$

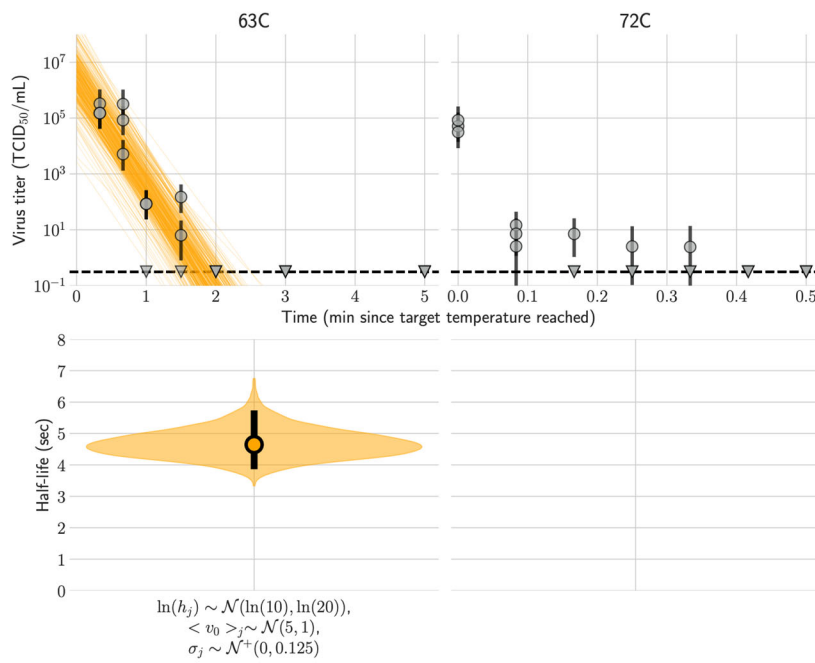
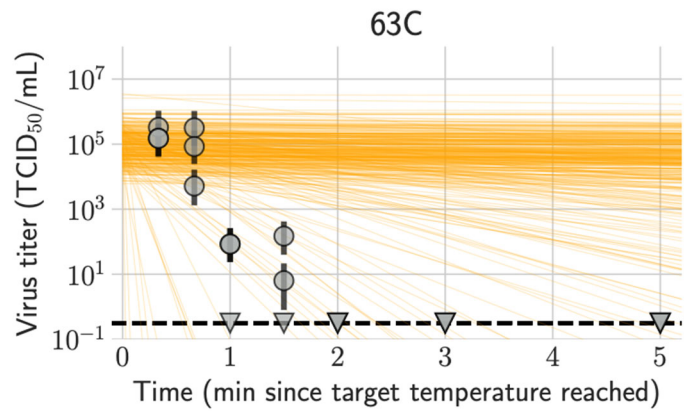


Figure S5: Prior predictive check and version of main text figure with first set of alternative half-life priors. Version of Figure S2 and main text figure, but with prior choices changed as indicated.



$$\ln(h_j) \sim \mathcal{N}(\ln(10), \ln(20)),$$

$$\langle v_0 \rangle_j \sim \mathcal{N}(5, 0.5),$$

$$\sigma_j \sim \mathcal{N}^+(0, 0.05)$$

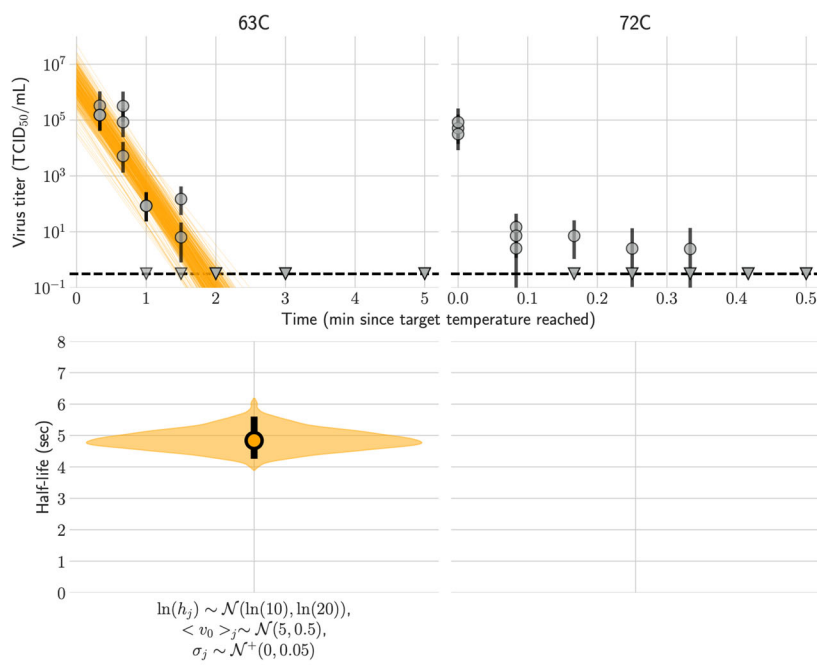
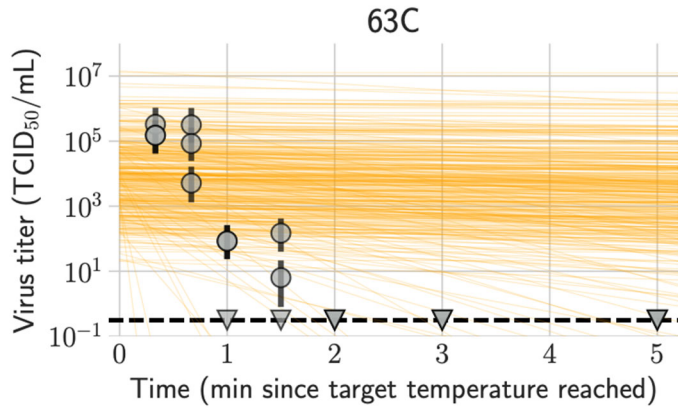


Figure S6: Prior predictive check and version of main text figure with first set of alternative half-life priors. Version of Figure S2 and main text figure, but with prior choices changed as indicated.



$$\ln(h_j) \sim \mathcal{N}(\ln(10), \ln(10)),$$

$$\langle v_0 \rangle_j \sim \mathcal{N}(4, 1),$$

$$\sigma_j \sim \mathcal{N}^+(0, 0.5)$$

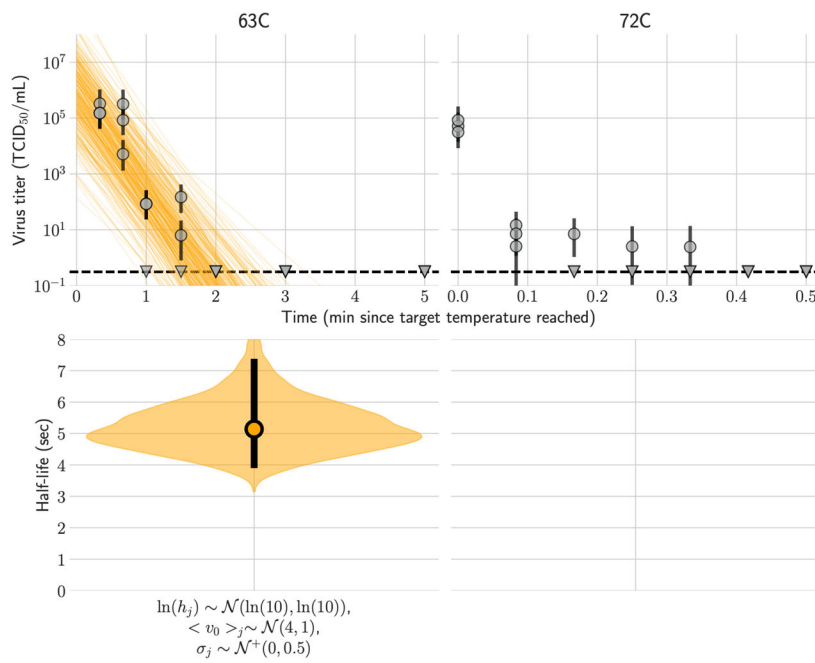


Figure S7: Prior predictive check and version of main text figure with first set of alternative half-life priors. Version of Figure S2 and main text figure, but with prior choices changed as indicated.

Supplemental Table

Figure and corresponding priors	Half-life (minutes)	Time for 10¹⁰-fold decrease (minutes)
main text	0.07 [0.06, 0.10]	2.45 [1.93, 3.21]
Fig. S3	0.07 [0.06, 0.10]	2.44 [1.92, 3.23]
Fig. S4	0.08 [0.07, 0.09]	2.56 [2.24, 2.95]
Fig. S5	0.08 [0.06, 0.10]	2.57 [2.14, 3.18]
Fig. S6	0.08 [0.07, 0.09]	2.68 [2.36, 3.10]
Fig. S7	0.09 [0.06, 0.12]	2.85 [2.16, 4.08]

Table S1: Sensitivity of results to specification of prior distributions. The table compiles posterior median and 95% credible intervals for the half-life of infectious H5N1 influenza virus in milk at 63 °C, and the corresponding time for the infectious virus titer to drop by a factor of 10¹⁰, for six different sets of prior distributions as defined for the six figures shown.

Supplemental references

1. Munster VJ, Baas C, Lexmond P, et al. Practical considerations for high-throughput influenza A virus surveillance studies of wild birds by use of molecular diagnostic tests. *J Clin Microbiol* 2009;47(3):666-73. DOI: 10.1128/JCM.01625-08.
2. Regulations CoF. Mandatory pasteurization for all milk and milk products in final package form intended for direct human consumption. (<https://www.ecfr.gov/current/title-21/chapter-I/subchapter-L/part-1240/subpart-D/section-1240.61>).
3. CEIRR. Attempted Influenza Virus Isolation From A(H5) RT-PCR Positive Supermarket Milk Samples. (<https://www.ceirr-network.org/news/attempted-influenza-virus-isolation-from-a-h5-rt-pcr-positive-supermarket-milk-samples>).
4. Gamble A, Fischer RJ, Morris DH, Yinda CK, Munster VJ, Lloyd-Smith JO. Heat-Treated Virus Inactivation Rate Depends Strongly on Treatment Procedure: Illustration with SARS-CoV-2. *Appl Environ Microbiol* 2021;87(19):e0031421. DOI: 10.1128/AEM.00314-21.
5. Phan D, Pradhan N, Jankowiak M. Composable Effects for Flexible and Accelerated Probabilistic Programming in NumPyro. *ArXiv* 2019;abs/1912.11554.
6. STAN. (<https://mc-stan.org/users/citations/>).

Acknowledgements

We would like to thank Erika Schwarz, Aracely Ospina Lopez, Nathaniel Antonioli, and Enrico Di Castro Young of the Molecular Diagnostics Section at the Montana Veterinary Diagnostic Laboratory, and Jennifer Ramsay and Matthew Becker of the Montana Fish, Wildlife & Parks wildlife health laboratory for their help with wildlife mortality surveillance. Sarah Anzick, Paul Beare, Kishore Kanakabandi of the NIAID RML research and technology branch for sequencing. Tessa Lutterman and Brandi Williamson for technical support. The authors declare no conflict of interests. DHM is an employee of the U.S. Centers for Disease Control and Prevention (CDC), but conducted this work in a personal capacity, as an uncompensated consulting scientist working with the JLS lab at UCLA. The findings and conclusions in this work do not necessarily represent the scientific positions of the CDC or the United States Government. This research was supported by the Intramural Research Program of the National Institute of Allergy and Infectious Diseases (NIAID), National Institutes of Health (NIH). JOL-S was supported by the U.S. National Science Foundation (DEB-2245631).